Int. J. Solids Structures Vol. 26, No. 3, pp. 331–351, 1990
Printed in Great Britain.

0020–7683/90 $3.00 + .00

SOME CHARACTERISTICS OF DISTRIBUTIONS OF FREE-EDGE INTERLAMINAR STRESSES IN COMPOSITE LAMINATES

LIN YE†
Department of Engineering Mechanics, Xian Jiaotong University, Xian, Shaanxi, P.R.C.

(*Received* 23 *September* 1988; *in revised form* 5 *June* 1989)

Abstract—Analyses of some characteristics of the distribution of interlaminar stresses near free edges in composite laminates are presented. First, results on the effect of the non-linear response of composite materials are presented. Emphasis is placed on identifying whether the linear elastic laminate model has sufficient accuracy in evaluations of interlaminar stress. Second, the singularity problem of interlaminar stresses is assessed by examining the dominant fields of singular stress potentials and the effective modulus concept. Third, characteristics of interlaminar stress distributions over the dimension of the fiber's diameter are discussed, based on a heterogeneous model, as well as the macroscopically homogeneous model. Finally, results of interlaminar stresses in composite laminates under bending are presented. These results will aid better understanding of the nature of free-edge interlaminar stresses in composite laminates, as well as the failure modes and failure process in laminated composite structures.

1. INTRODUCTION

Interlaminar stress in a composite laminate near its geometric boundaries, has been a subject of intensive investigation during the last two decades. Both experimental studies and analytical solutions have indicated that complex stress states with a rapid change of gradients occur along the edges of composite laminates. The occurance of interlaminar stresses is considered to result from the presence and interactions of geometric discontinuities of the composite laminate and material discontinuities through the laminate thickness. Interlaminar stress has been found to occur only within a very local region near the geometric boundaries of a composite laminate, and is frequently referred to as a "free edge effect". The high interlaminar stresses coupled with the low interlaminar strength have been found to be of critical significance in the failure of laminated composite structures.

The first approximate solution of interlaminar stresses was proposed by Puppo and Evensen (1970), based on a laminate model with interlaminar normal stress being neglected in the laminate. The approach, which consisted of three interlaminar stress components, was first made by Pipes and Pagano (1970). From then on, analysis of interlaminar stresses was a very active field of study. A great variety of methods have been proposed to calculate interlaminar stress. The representative methods are: the finite difference method by Pipes and Pagano (1970), the boundary layer theory by Tang and Levy (1975), the finite element method by Wang and Crossman (1977), the Raleigh–Ritz method by Pagano (1978), the hybrid finite element methods by Spilker and Chou (1980) and Wang and Yuan (1983), the complex variable stress potentials by Wang and Choi (1982b), and the Global–Local model by Pagano and Soni (1983).

Wang and Crossman (1977) suggested from analysis of their finite element results that there might be a singularity in the distributions of interlaminar stress at the corner of the free-edge interface, and the singularity of interlaminar stresses then became the focus of attention. The systematic convergence studies by Raju and Crews (1981) appeared to confirm the existence of a stress singularity at the intersection of the interface and the free edge. Wang and Choi (1982a) and Ting and Chou (1981a,b), separately, obtained the singular orders of interlaminar stresses successfully through the complex-variable stress potentials of the anisotropic linear elasticity. However, Bar-Yoseph and Pian (1981) believed there is no singularity in interlaminar stresses near free edges.

† Formerly at Beijing Institute of Aeronautics and Astronautics, Beijing, P.R.C.

Summing up the review, many significant results have been obtained on analysis of interlaminar stresses near free edges in composite laminates, during the past two decades. However, due to the complexity of the problem, there are still some characteristics which need further detailed identification. One is the effect of the non-linear response of epoxy matrix resin composites on interlaminar stress distributions. A question that should be answered is whether the linear elastic model is accurate enough for evaluation of interlaminar stresses. Another refers to the influence of the strength of the singularity on the physical extent of the free-edge stress gradients. The inter-relationship of homogeneous and heterogeneous material property assumptions is a key to explore the nature of the stress singularity. A rational analysis of the problem directly affects what kind of model should be used to characterize delamination onset from free edge in composite laminates. Next, in the previous investigations, the laminate model was mostly restricted to one bound by a cylindrical edge surface and subjected to uniform end tractions. The flexural or flexural–extension coupling characteristics of the laminate were ignored. However, these characteristics aid better understanding of the failure modes and failure process of laminated composite structures.

In the following sections, analysis of some characteristics of interlaminar stress distributions which were scarcely mentioned in the open literature are presented. It includes: (1) the effect of non-linear response of composite materials; (2) the dominant field of singular stress and effective modulus concept; (3) the effect of material heterogeneity; (4) interlaminar stresses in composite laminates under bending.

2. LAMINATE MODEL

Consider a composite laminate (Fig. 1) bound by a cylindrical edge surface and subjected to surface tractions acting on planes normal to the generator of the end lateral surfaces. The laminate is assumed to be sufficiently long so that the end effect is neglected by virtue of Saint-Venant's principle in the region far from the ends. Consequently, the stress state in the composite laminate is independent of the x-variable.

The following basic assumptions were used: (1) the material in each layer is a macroscopically homogeneous and orthotropic body; (2) small deformations and an initially stress-free field with neglected body force are assumed. The first assumption implies that the material properties of a composite layer are represented by a group of "effective moduli" of a representative material element with a finite volume and consisting of fibers and matrix.

Following the procedure in the theory of anisotropic elasticity (Lekhnitskii, 1963), the general expressions for displacements and the stress component σ_x have the following forms,

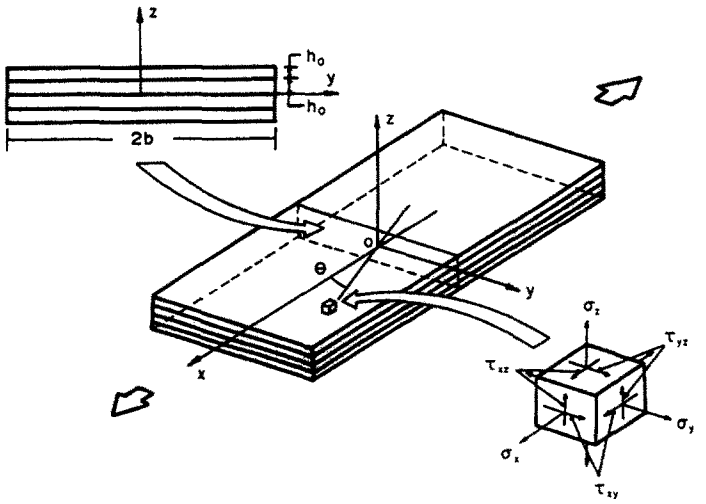

Fig. 1. Geometry and coordinates of the laminate model.

$$u = (C_1 y + C_2 z + C_3) S_{11} x + U(y,z)$$
$$v = -\tfrac{1}{2} C_1 S_{11} x^2 - C_4 z x + V(y,z)$$
$$w = -\tfrac{1}{2} C_2 S_{11} x^2 + C_4 y x + W(y,z)$$
$$\sigma_x = C_1 y + C_2 z + C_3 + S_{ij}\sigma_j / S_{11} \quad (j = 2,\ldots,6) \tag{1}$$

where unknown functions U, V and W only depend on variables y and z. Coefficients C_1 and C_2 respectively represent the bending of the laminate in the x–y and x–z planes. C_3 characterize the uniform axial extension of the composite laminate, and C_4 the relative angle of rotation about the z-axis.

3. EFFECT OF NON-LINEAR RESPONSE OF COMPOSITES

For fiber-reinforced epoxy resin composites, only the properties in the fiber direction can be considered to be linear elastic. The transverse normal, transverse shear and longitudinal shear responses are dominated by the matrix resin, and they are of obvious non-linear behavior. The shear response is even significant at very low load levels.

Shown in Fig. 2 are the stress–strain cycles increased progressively in the quasi-static tension tests, obtained by the author (Ye, 1987) for T300/648·BF_3MEA and T300/634·DDS graphite/epoxy $(\pm 45)_{4s}$ composite laminates. It can be seen that the material responses have significant non-linear behavior. Additionally, although there are plastic strains under small deformations, the materials mainly have non-linear elastic deformations. Hence, the modified two-dimensional Hahn–Tsai's (Hahn and Tsai, 1973) non-linear elastic constitutive equations, implemented by Xia *et al.* (1986), are extended to the three-dimensional case, by assuming the material in the plane normal to fibers to be isotropic,

$$\sigma_i = S_{ij}\varepsilon_j \quad (i,j = 1,2,\ldots,6) \tag{2}$$

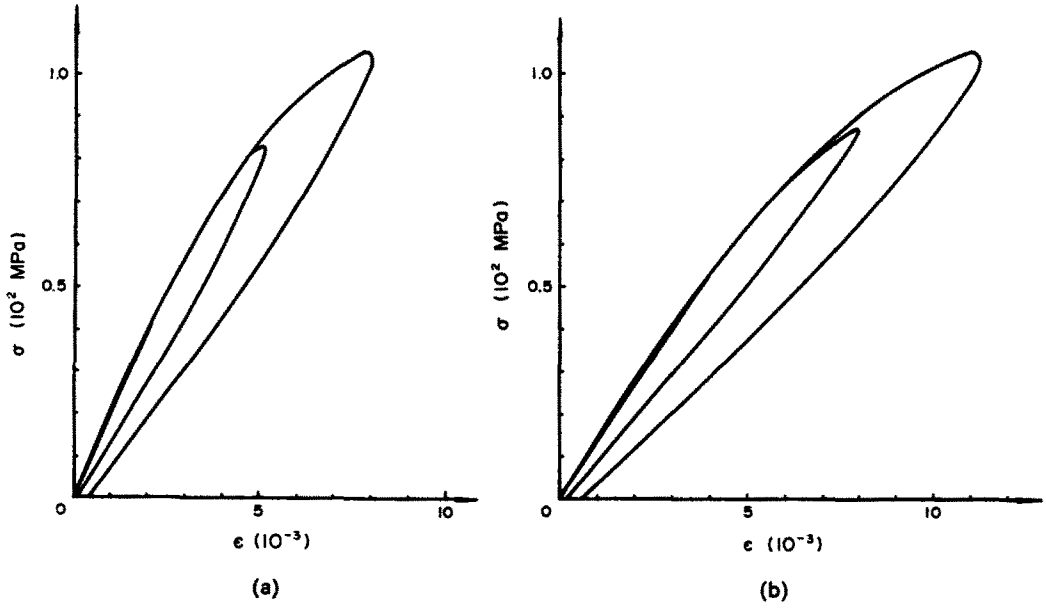

Fig. 2. Stress–strain cycles increased progressively for T300/648 and T300/634 graphite/epoxy $(\pm 45)_{4s}$ composite laminates.

where

$$\{S_{ij}\} = \begin{bmatrix} \frac{1}{E_{11}} & -\frac{\nu_{12}}{E_{11}} & -\frac{\nu_{13}}{E_{11}} & 0 & 0 & 0 \\ & S_{22} & -\frac{\nu_{23}}{E_{22}} & 0 & 0 & 0 \\ & & S_{33} & 0 & 0 & 0 \\ & \text{sym} & & S_{44} & 0 & 0 \\ & & & & S_{55} & 0 \\ & & & & & S_{66} \end{bmatrix} \tag{3}$$

and

$$S_{22} = \frac{1}{E_{22}} + S_{2222}\sigma_2^2 \quad S_{33} = \frac{1}{E_{33}} + S_{3333}\sigma_3^2$$

$$S_{44} = \frac{1}{G_{23}} + S_{4444}\tau_{23}^2 \quad S_{55} = \frac{1}{G_{13}} + S_{5555}\tau_{13}^2$$

$$S_{66} = \frac{1}{G_{12}} + S_{6666}\tau_{12}^2 \tag{4}$$

where subscripts 1, 2 and 3 refer to the fiber direction, transverse normal and thickness directions of a composite lamina.

For convenience, only the composite laminate under uniform extension is considered here. From the symmetric and non-symmetric conditions of deformations, and the axial strain $\varepsilon_x = \varepsilon_0$ under uniform extension, the following coefficients can be obtained,

$$C_1 = C_2 = C_4 = 0 \tag{5}$$

$$C_3 = \varepsilon_0 / S_{11} \tag{6}$$

then the displacements in the laminate can be expressed as,

$$u = \varepsilon_0 x + U(y, z)$$
$$v = V(y, z)$$
$$w = W(y, z). \tag{7}$$

A quasi-three-dimensional finite element method which is similar to the method by Wang and Crossman (1977) was used in the present analysis. Due to the presence of non-linear behavior of stress–strain relations, a system of non-linear algebraic equations is obtained from the finite model,

$$\mathbf{K}(\boldsymbol{\varphi})\boldsymbol{\varphi} - \mathbf{F}(\boldsymbol{\varphi}) = \mathbf{0}. \tag{8}$$

Let

$$\boldsymbol{\psi}(\boldsymbol{\varphi}) = \mathbf{K}(\boldsymbol{\varphi})\boldsymbol{\varphi} - \mathbf{F}(\boldsymbol{\varphi}). \tag{9}$$

Assuming $\boldsymbol{\varphi}_n$ to be the nth alternative value, in general cases,

$$\boldsymbol{\psi}(\boldsymbol{\varphi}_n) \neq \mathbf{0}. \tag{10}$$

We also assume the $(n+1)$th alternative values $\boldsymbol{\varphi}_{n+1}$ to satisfy eqn (8), that is,

$$\boldsymbol{\varphi}_{n+1} = \boldsymbol{\varphi}_n + \Delta\boldsymbol{\varphi}_n \tag{11}$$

$$\psi(\varphi_n+\Delta\varphi_n) = \mathbf{0}. \tag{12}$$

Taking the first-order expansions of ψ near φ_n, we have

$$\psi(\varphi_n)+\nabla\psi(\varphi_n)\Delta\varphi_n = \mathbf{0} \tag{13}$$

$$\nabla\psi(\varphi_n) = \mathbf{K}(\varphi_n)+\nabla\mathbf{K}(\varphi_n)\varphi_n+\nabla\mathbf{F}(\varphi_n). \tag{14}$$

Due to the calculations of $\nabla\mathbf{K}(\varphi_n)$ and $\nabla\mathbf{F}(\varphi_n)$ being very complicated, the last two terms in eqn (14) are ignored, that is

$$\nabla\psi(\varphi_n) = \mathbf{K}(\varphi_n). \tag{15}$$

For further simplification, $\mathbf{K}(\varphi_n)$ can be taken to be the first values $\mathbf{K}(\varphi_0)$, which is the stiffness matrix determined from the linear elastic model. The final alternative equations are,

$$\mathbf{K}(\varphi_0)\Delta\varphi_n = -\psi(\varphi_n) \tag{16}$$

$$\psi(\varphi_n) = \int\int \bar{\mathbf{B}}^{\mathrm{T}}\bar{\mathbf{C}}\bar{\varepsilon}\,\mathrm{d}A-\int\int \bar{\mathbf{B}}^{\mathrm{T}}\bar{\mathbf{C}}\bar{\varepsilon}_0\,\mathrm{d}A \tag{17}$$

$$\varphi_{n+1} = \varphi_n+\Delta\varphi_n \tag{18}$$

where $\bar{\mathbf{B}}$ and $\bar{\mathbf{C}}$ are the simplified geometric and stiffness matrices which can be found in Wang and Stango (1983), and $\bar{\varepsilon}_0$ is the simplified initial strain vector. When $(\|\varphi_{n+}-\varphi_n\|)/\|\varphi_n\| \leqslant \mathrm{Tol}$, the results can be considered to have converged.

By convention, angle-ply $(45/-45)_s$, cross-ply $(0/90)_s$ and $(90/0)_s$ composite laminates are examined. The geometric configuration is the same as that in Wang and Crossman (1977). The material properties for T300/634·DDS graphite/epoxy composite, with non-linear elastic behavior (Fig. 3), are chosen in the analysis. Material and geometric symmetry conditions permit that only one quarter of the laminate cross-section be examined. Eight-noded quadrilateral isoparametric elements are used. There are in total 180 elements and 597 nodes (Fig. 4 shows the finite element mesh). In the analysis, $\varepsilon_0 = 10^{-2}$, and the convergent coefficient, $\mathrm{Tol} = 10^{-4}$. For the three laminates, there is only one alternation for convergence.

In order to assess the effect of non-linear response of the material on interlaminar stress distributions, the results for a linear elastic model [the non-linear terms in eqn (4)

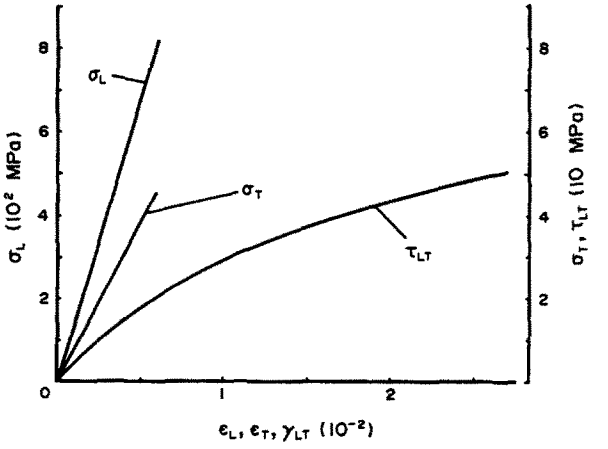

Fig. 3. Lamina properties for T300/634 composite material.

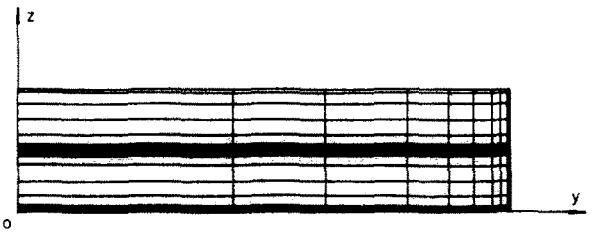

Fig. 4. Finite element mesh.

are assigned to be zero] are also presented. In addition, non-dimensional stresses are used in the discussion, that is, $\sigma_{ij}^* = \sigma_{ij}/\sigma_0$. σ_0 is the average axial stress,

$$\sigma_0 = \frac{1}{A}\iint_A \sigma_x \, dA \tag{19}$$

where A is the area of the laminate cross-section. In this way, comparisons of interlaminar stresses distributions in the non-linear elastic model with those in the elastic model can be made.

For $(45/-45)_s$ laminate, the average axial stress σ_{0n} of the non-linear elastic model, under the present axial strain ε_0, differs significantly from σ_{0e} of the elastic model; $\sigma_{0n}/\sigma_{0e} = 0.59$. This result indicates that the axial stiffness, considering the non-linear response of the material, is decreased by 41% compared with that of the elastic model. The non-linear response of the material has a significant effect on the stiffness of $(45/-45)_s$ laminate.

Shown in Fig. 5 is the distribution of interlaminar normal stress σ_z along $45/-45$ interface. σ_z presents a compressive behavior near the free edge. The absolute value of σ_z of the non-linear elastic model is slightly larger than that of the elastic model, but it is difficult to distinguish the difference in drawing precision at most locations. Figure 6 shows the through-thickness distribution of shear stress τ_{xz} near the free edge. The existence of τ_{xz} is one major factor causing interlaminar shear failure. Shear stress τ_{xz}, considering the non-linear response of the material, also has an evident stress concentration at the $45/-45$ interface. However, its distributive value is smaller than that of the elastic model. Figure 7 shows the distribution of axial displacement U along the upper boundary of the laminate cross-section, which represents the bent degree of the laminate cross-section under loading.

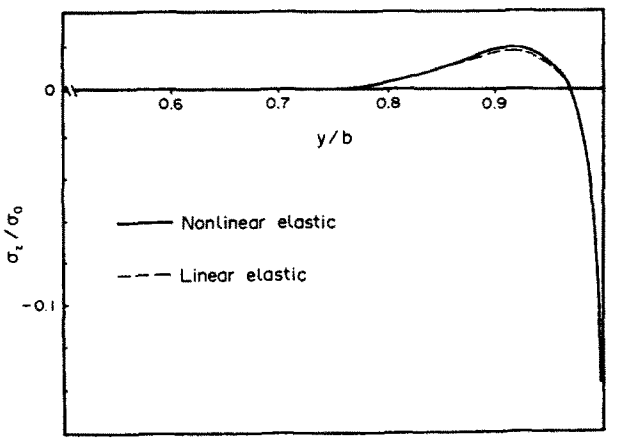

Fig. 5. Distribution of interlaminar normal stress σ_z along $45 -45$ interface in $(45/-45)_s$ laminate.

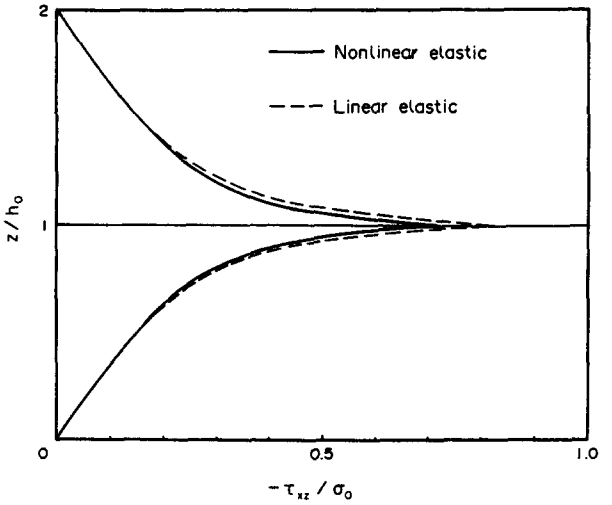

Fig. 6. Through-thickness distribution of τ_{xz} near the free edge ($y/b = 0.997$) in $(45/-45)_s$ laminate.

It can be seen that the section bent degree of the non-linear elastic model is larger than that of the elastic model, which means the elastic model can overestimate the section stiffness.

For $(0/90)_s$ and $(90/0)_s$ laminate, the average axial stresses of the non-linear elastic model have no evident differences compared with those of the elastic model; both $\sigma_{0n}/\sigma_{0e} = 0.998$. This result indicates that for cross-ply laminates, the axial laminate stiffness is almost identical.

Shown in Fig. 8. and Fig. 9 are the distributions of interlaminar normal stress σ_z along the 0/90 interface and the midplane in the cross-ply laminates. Considering the non-linear response of the material, the absolute value of σ_z of the non-linear elastic model is slightly smaller than that of the elastic model, and it is difficult to distinguish the difference between them. Figure 10 shows the distributions of interlaminar shear stress τ_{yz} along the 0/90 interface. It can be seen that the distributive value of τ_{yz} of the non-linear elastic model is smaller than that of the elastic model.

By summarizing the present results, the following points can be drawn: the existence of non-linear response of materials may cause the structural stiffness of composite laminates

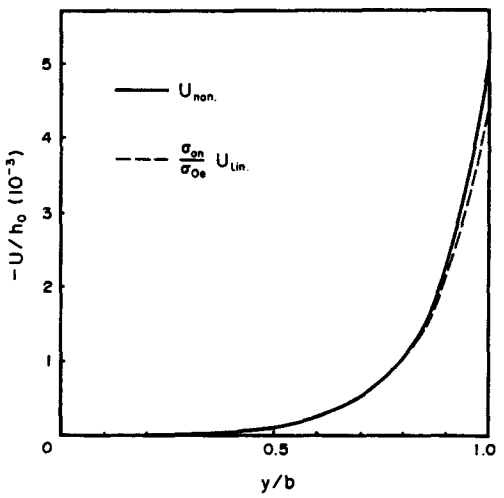

Fig. 7. Distribution of axial displacement U along the upper boundary ($z = 2h_0$) of $(45/-45)_s$ laminate cross-section.

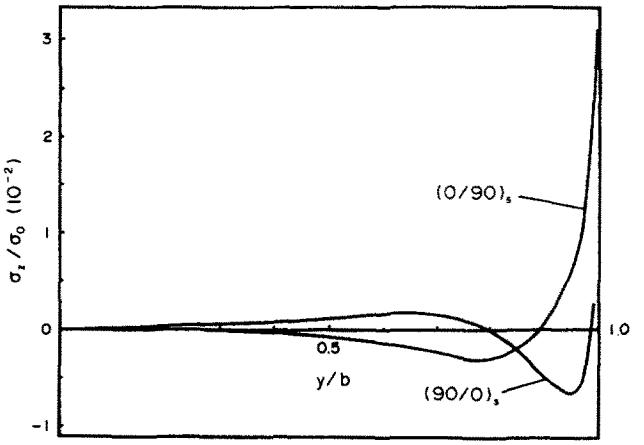

Fig. 8. Distributions of interlaminar normal stress σ_z along 0/90 interface in $(0/90)_s$ and $(90/0)_s$ laminates.

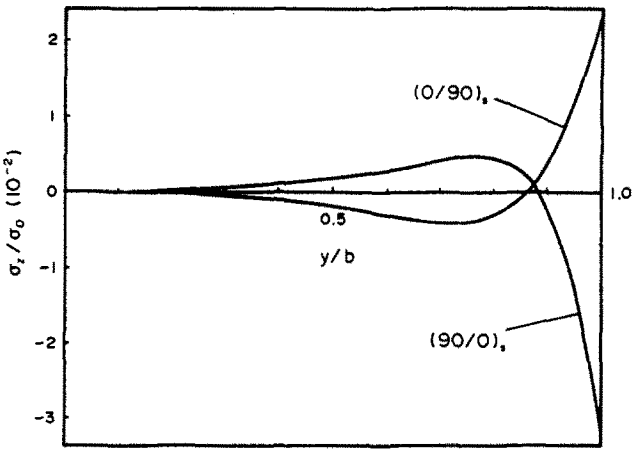

Fig. 9. Distributions of interlaminar normal stress σ_z along the midplane in $(0/90)_s$ and $(90/0)_s$ laminates.

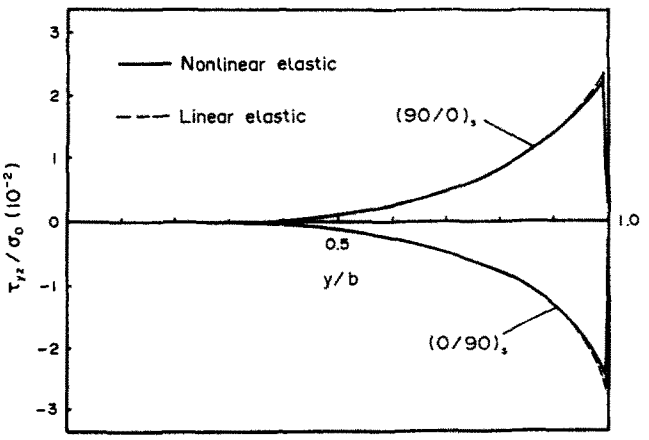

Fig. 10. Distributions of interlaminar shear stress τ_{yz} along 0/90 interface in $(0/90)_s$ and $(90/0)_s$ laminates.

to be smaller than that estimated by the elastic model, in varying degrees; considering the non-linear response of materials, the distributions of interlaminar stresses have almost the same features as those of the linear elastic model, and interlaminar stresses also have significant stress concentration near the free edge; under small deformations, the presence of a non-linear response of materials can reduce the stress concentration of interlaminar shear stresses to a certain degree, but it has little effect on interlaminar normal stress. This point means that the linear elastic model can be used to evaluate the distributions of interlaminar stresses in composite laminates without an evident loss of accuracy.

4. PROBLEM OF SINGULARITY OF INTERLAMINAR STRESS

4.1. *The order of singularity*

Under the assumption that each layer in a composite laminate is a macroscopically homogeneous, orthotropic and linear elastic body, the order of singularity of interlaminar stresses can be obtained based on the theory of anisotropic elasticity and the complex-variable stress potentials. Considering the complex-variable expansions of displacements and stresses, and by applying the stress-free boundary conditions and the interface continuity conditions of stresses and displacements, a system of 12 linear homogeneous equations can be obtained. The order of stress singularity of the singular terms in stress expansions can be achieved by solving an eigenvalue problem. The details can be found in Wang and Choi (1982a) and Ting and Chou (1981a,b). Under the coordinate system shown in Fig. 11, the singular terms of stresses expansions can be expressed as,

$$\sigma_{ij} = K_{ij}^{*} r^{\delta} \sigma_{ij}^{*}(\varphi) \quad (i, j = 1, 2, 3) \tag{20}$$

where $\sigma_{ij}^{*}(\varphi)$ only are functions of φ. δ is a negative constant, and is the order of the singularity, which depends only on material elastic constants and fiber orientations of adjacent plies in a composite laminate. K_{ij}^{*} can be considered as the analogy of the stress intensity factors in the linear elastic fracture mechanics (Sih and Liebowitz, 1968), and they depend on the stacking sequence of the layers and the complete boundary conditions.

Shown in Fig. 12 are the singular orders of interlaminar stress expansions near the free edge between two $\theta/0$, $\theta/90$ and $\theta/-\theta$ adjacent layers, which were drawn from the results of Ting and Chou (1981a). It can be seen that the strength of the singularity of the interlaminar stresses is quite weak. From the analytical results of Wang and Choi (1982a), Ting and Chou (1981a,b) and Zwiers *et al.* (1982), for graphite/epoxy composites, the strength of the singularity of the interlaminar stresses is smaller by at least one order, than that of the $-\frac{1}{2}$ singular order of stresses in the vicinity of a crack tip in the linear elastic fracture mechanics.

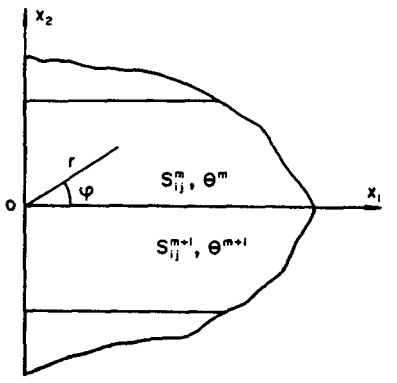

Fig. 11. The interface near the free edge in a composite laminate.

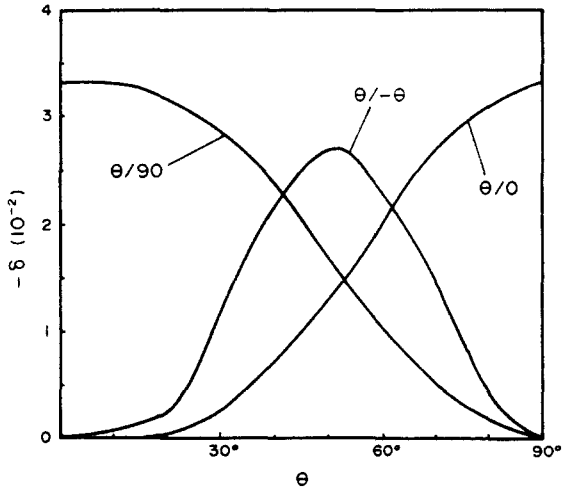

Fig. 12. Singular orders of interlaminar stress near free edge between two $\theta/0$, $\theta/90$ and $\theta/-\theta$ adjacent layers drawn from the results of Ting and Chou (1981a).

From linear elastic fracture mechanics (Sih and Liebowitz, 1968), the singular terms of stress expansions for a Mode-I crack in the plane problem (Fig. 13) can be expressed as,

$$\sigma_{x\beta} = \frac{K}{\sqrt{2\pi r}}\sigma^{*}_{x\beta}(\varphi) \quad (\alpha, \beta = 1, 2). \tag{21}$$

Generally, for the crack problem with the $-\frac{1}{2}$ singular order, the singular terms, eqn (21), of stress expansions can well approach the exact solutions, when $r/a \leqslant 0.1$ (a is the crack length). Hence, eqn (21) is widely used to determine the small plastic zone in the vicinity of a crack tip, and is used to generate the stress intensity factors with the finite element method in the fracture mechanics.

In order to discuss the dominant field of the singular terms of interlaminar stresses, distributions of two stress potentials, $\sigma_1(r) = Kr^{-0.05}$ with a -0.05 order of singularity, and $\sigma_2(r) = Kr^{-0.5}$ with a -0.5 order of singularity, are illustrated in Fig. 14. If $\sigma_2(r)$ is assumed to be the stress ahead of a crack tip, it can be taken as an analogy to eqn (21). Then its dominant field is $r/\alpha \leqslant 0.1$. However, the scope of $\sigma_1(r)$ with the same order value is $r/a \leqslant (0.1)^{10} = 10^{-10}$. Therefore, it can be inferred that the dominant field of singular terms of interlaminar stresses in composite laminates is smaller by at least ten orders, than that of stresses ahead of a crack tip in the linear elastic fracture mechanics, if "stress intensity factors" are of the same order.

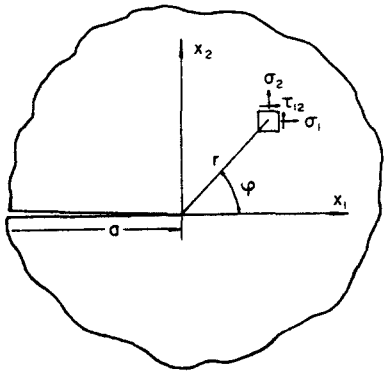

Fig. 13. A Mode-I crack in a plate body.

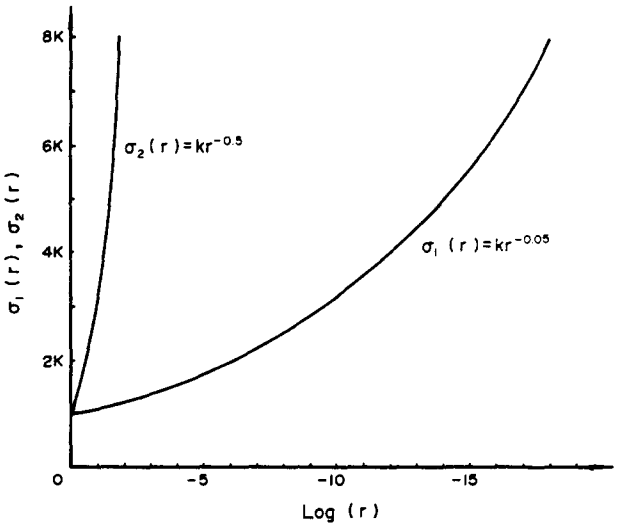

Fig. 14. Distributions of singular stress potentials.

It is frequently considered that interlaminar stresses in a composite laminate only exist in the region with a dimension of a laminate thickness to the free edge. Hence, the dominant field of singular terms of interlaminar stresses can be several orders smaller than the dimension of the fiber diameter (7×10^{-3} mm generally for graphite fibers).

During the last decade, some analytical solutions which did not consist of the singularity of interlaminar stresses were developed by Wang and Dickson (1978) and Loo (1986). The stresses were expanded in the Legendre series or the Fourier series, and the convergence of these series was quite rapid. From this phenomenon, it can be considered that the effect of singular terms is within the scale of the critical convergent coefficient. Using this meaning. the effect of singular terms of interlaminar stresses can be ignored.

4.2. *Effective modulus concept*

In order to determine the macroscopic response of composite materials, the assumption that a composite is a macroscopically homogeneous body must be made. As the basic assumption in the previous section, heterogeneous (fiber/matrix) composite layers are treated as homogeneous and orthotropic materials, and their material properties are characterized by those of the representative volume element of the composite. This effective modulus representation for composite materials is widely used in the stress analysis and design of structural composite laminates. However, this approach, as pointed out by Pagano and Rybicki (1974, 1975), breaks down in the presence of a non-uniform macroscopical stress field. Through a modified effective modulus approach, they indicated that the effective modulus stress field cannot predict the correct physical response and that interpreting the field values (point by point) of the effective modulus stresses may lead to erroneous conclusions. Hence, the physical significance of effective modulus solutions, as well as the ranges of validity of them, should be further examined.

The inter-relationship of homogeneous and heterogeneous material property assumptions is a key to understanding the physical response of composite materials. A great variety of models have been developed to correlate the properties of a composite material (a lamina) and those of its constituents (fiber/matrix). A detailed review can be found in Jones (1975) and Christensen (1979). Most approaches just took a representative volume element, e.g. the model of a cylindrical matrix embedded with a cylindrical fiber (Whitney and Riley, 1966) to represent a composite. Strictly speaking, there is some difference between those models and the real composites, regarding their physical behavior.

The approach by Liu (1984) used a more rational way to establish the model. It started with a composite body by assuming that a composite is formed by adding fibers one by one

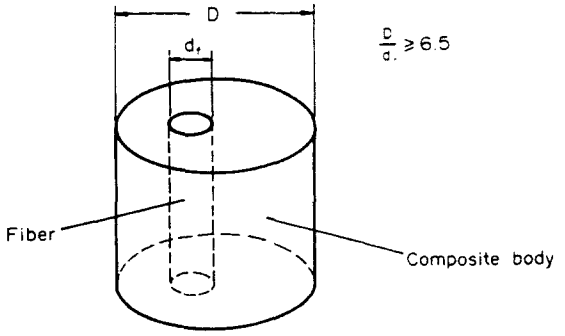

Fig. 15. Valid dimension of effective modulus representation for composites.

to a matrix body. When a fiber is being put in, a composition procedure is undergone, which can be described by the model of Whitney and Riley (1966), and a new matrix body forms. Then, the properties of a composite can be obtained when the properties converge and the constituent volume fractions reach the real values. As in the model indicated in Fig. 15, D is the overall dimension of the composite body, and d_f is the real dimension of fibers. When the volume fraction is determined, the ratio of D/d_f is directly related to the alternative number. It was found the properties of a composite do not change when the ratio of D/d_f is over a certain value. This value can be considered to be a critical one to distinguish a composite body in a homogeneous scale from that in a heterogeneous scale. When D/d_f is smaller than this value, the composite body cannot be taken as a macroscopically homogeneous one and should be treated as a microstructure. As indicated by Liu, the minimum dimension of a composite body, over which the effective modulus representation for composite materials is valid, should be 6.5 times greater than that of the fiber diameter, for glass/epoxy and graphite/epoxy composites in the range of fiber volume fraction $0.3 \leqslant V_f \leqslant 0.7$. For graphite/epoxy composite materials, this definite dimension is in 0.045 mm scale, and is almost equal to one third of a typical thickness of a composite layer (0.125 mm).

When using the macroscopically homogeneous model to determine interlaminar stresses and other mechanical responses in composite materials, the dimensions over which the effective modulus solutions are valid should be considered. Within the dimension order of the fiber diameter, there is little meaning, point by point, to discuss the stress distributions evaluated with the macroscopically homogeneous model. It has been pointed out that the dominant field of singular terms of interlaminar stresses can be smaller by several orders than the dimension of the fiber diameter. In addition, in practical laminates there is no material discontinuity through the interface, and the artificial discontinuity is caused by the effective modulus approach. Hence, a point can be drawn: the singularity of interlaminar stresses near free edges results from the homogenized assumption for composite materials, and it is more rational to use the stress concentration concept to characterize the nature of interlaminar stresses near the free edge.

5. THE EFFECT OF MATERIAL HETEROGENEITY

Many solutions of the macroscopically homogeneous model for interlaminar stresses indicated that there is a rapid change of gradients near free edges over the dimension of several times the fiber diameter. It has been pointed out that over this dimension the asumption that composite materials are homogeneous no longer holds, and the effective modulus concept is not valid. Hence, it is necessary to examine the characteristics of interlaminar stresses in this scale. In this work, $(0/90)_s$ and $(90/0)_s$ symmetric cross-ply composite laminates under uniform extension are examined. In brief, the results for $(0/90)_s$ laminate are presented.

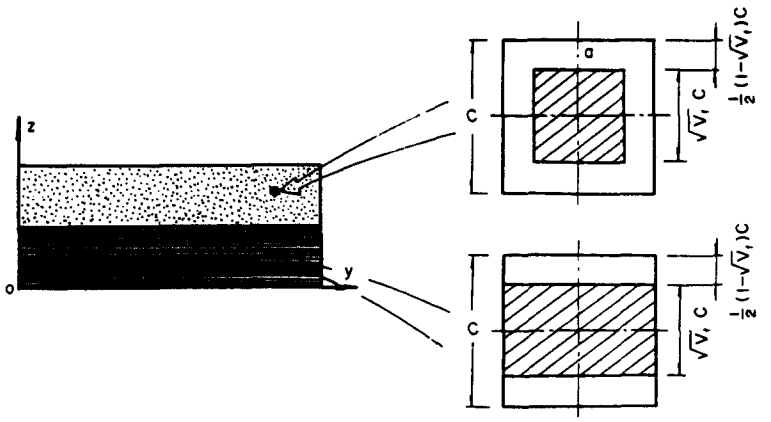

Fig. 16. Representative volume elements for the heterogeneous laminate model.

For fiber-reinforced composite materials, the matrix resins are generally considered to be isotropic, and fibers transversely isotropic. Since only 0-deg and 90-deg plies are incorporated in the laminate, there is a material symmetric plane parallel to the y–z plane in each layer. Hence, we have $\gamma_{xz} = \gamma_{xy} = 0$. The displacements in the laminate can be simplified as,

$$u = \varepsilon_0 x \qquad v = V(y,z) \qquad w = W(y,z). \tag{22}$$

In composite layers, the distribution of fibers in matrix resins is generally random. For convenience of analysis, simplification of the physical model must be made. In the analysis, two representative volume elements in the form of a square prism are assumed for 0-deg and 90-deg plies, respectively (Fig. 16). In the elements, a fiber embeds in a matrix block, and the fiber and matrix are considered to be a perfect bond. The array of fibers in 0-deg plies is assumed to be square arrangement and fibers are assumed to have a rectangular cross-section. As shown in Fig. 16, the relative dimensions of the fiber and matrix can be determined from the volume fractions. Hence, a layer (0-deg or 90-deg) in cross-ply composite laminates is considered to be a composite of a lot of corresponding representative volume elements.

As for the properties of fibers, the material constants for T300 graphite fiber are taken from the open literature,

$$E_f = 210\,(\text{GPa}) \quad E_T = 14.5\,(\text{GPa}) \quad G_f = 14.5\,(\text{GPa}) \quad \nu_f = 0.3 \quad \nu_{fT} = 0.4$$

where T refers to the transverse normal direction of a fiber. For the properties of the matrix resin, the material constants are chosen for an epoxy resin, 648/BF_3 MEA in applications.

$$E_m = 3.14\,(\text{GPa}), \qquad \nu_m = 0.35.$$

A finite element method was used in the analysis, and eight-noded quadrilateral isoparametric elements were used. Dimensions and geometry of the laminate are: $b = 100$ μm; $h_0 = 40$ μm. The thickness of each layer is almost one third of the thickness (0.125 mm) of a real composite layer, and corresponds to the minimum dimension over which the effective modulus concept is valid. Material and geometric conditions permit that only one quarter of the laminate cross-section be examined (Fig. 17a shows a finite element mesh corresponding to the representative volume elements). The dimension of a representative volume element is $c^2 = 10 \times 10\,\mu\text{m}^2$. Taking the fiber volume fraction, $V_f = 0.64$, the dimension of the fibers is $a = 8$ μm.

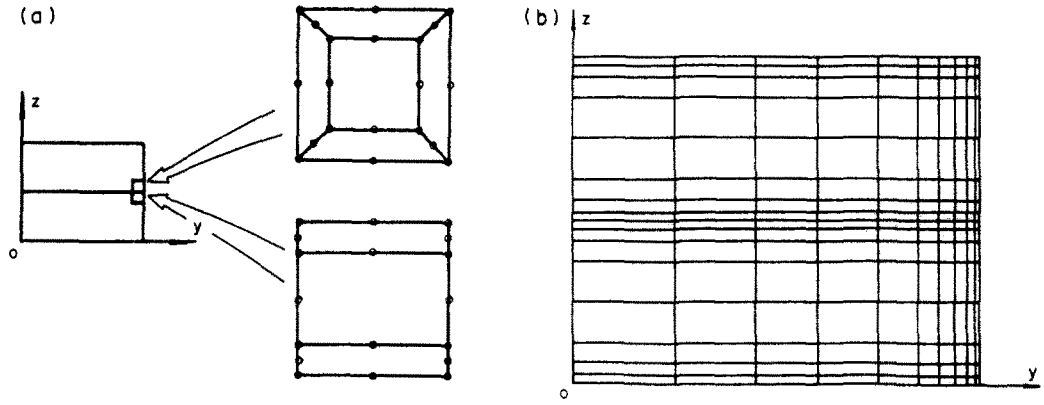

Fig. 17. Finite element mesh, (a) heterogeneous model, (b) homogeneous model.

In order to assess the effects of material heterogeneity on the distributions of interlaminar stresses, results for the corresponding homogeneous model are also presented (Fig. 17b shows a finite element mesh). The Tsai–η method by Tsai and Hahn (1980) was used to predict the lamina properties from the fiber and matrix properties.

For the heterogeneous model, the macroscopic interface does not exist between two adjacent layers. For the convenience of comparison with the results of the homogeneous model, emphasis is still placed on assessing the distributions of interlaminar stresses at the macroscopic interface.

Shown in Fig. 18 is the distribution of interlaminar normal stress σ_z along the 0/90 interface. It can be seen that there are evident differences between the characteristics of stress distributions of the two models. However, for both models, the significant stress concentration exists near the free edge. Due to the effect of heterogeneity, the stress distribution of the heterogeneous model represents an oscillatory behavior. At the location just under a fiber in 0-deg ply, the stress value is obviously smaller than its average trend. This phenomenon is due to the fact that the transverse normal modulus of the fiber is obviously greater than that of the matrix resin (about 4.6 times), and the matrix deformations around a fiber are restrained by the fiber. Additionally, it can be found that the average trend of the stress distribution of the heterogeneous model is very close to the stress distribution of the homogeneous model. Figure 19 shows the distribution of interlaminar normal stress σ_z along the midplane ($z = 0$). Since the midplane is just under a fiber parallel to the y-axis, the arrangement of fibers has little effect on the stress distribution. It can be

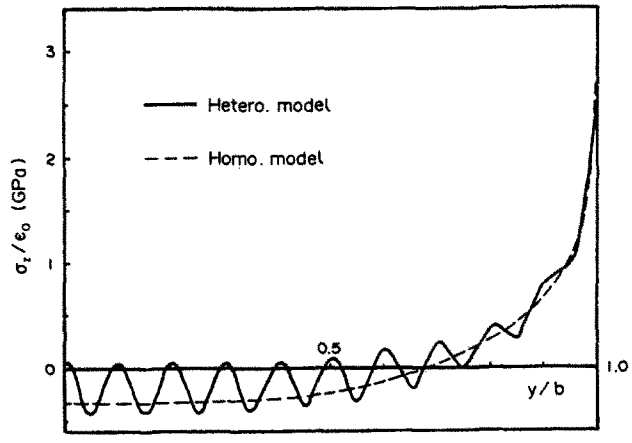

Fig. 18. Distribution of interlaminar normal stress σ_z along 0/90 interface in (0/90)$_s$ laminate.

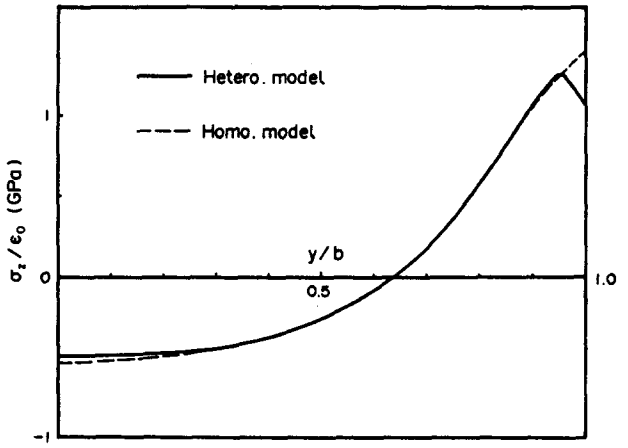

Fig. 19. Distribution of interlaminar normal stress σ_z along the midplane in $(0/90)_s$ laminate.

seen that the stress distribution of the heterogeneous model is finely close to that of the homogeneous model, and it is believed that the difference in stress distributions near the free edge is caused by the coarse mesh of the heterogeneous model. In Fig. 18 and Fig. 19, σ_z has not approached zero at the location $y/b = 0$, which implies that the laminate is not wide enough. When the laminate has sufficient width, σ_z will approach zero.

Shown in Fig. 20 and Fig. 21 are the through-thickness distributions of σ_z at the free edge and the location, $y/b = 0.9$. In the 90-deg ply, σ_z obtained with the heterogeneous model has an oscillatory distribution, but its average trend is very close to the stress distribution of the homogeneous model. In the 0-deg ply, the distributions of σ_z in both models are almost the same. At the location $y/b = 0.9$, there is a difference between the stress distributions of the two models in the area close to the interface. In the other region, the results of the two models are very close to each other.

Summarizing the discussion, the present results indicate that the effect of material heterogeneity on the distributions of interlaminar stress is significant over the dimension of several times the fiber diameter. However, the average trend of interlaminar stress distributions of the heterogeneous model is very close to the stress distribution of the homogeneous model. Additionally, for the heterogeneous model, interlaminar stresses also have significant stress concentration near the free edge. Though the heterogeneous model exam-

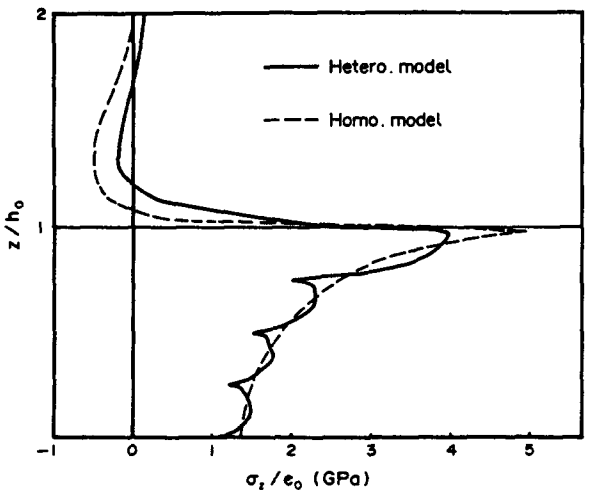

Fig. 20. Through-thickness distribution of σ_z at the free edge ($y/b = 1$) in $(0/90)_s$ laminate.

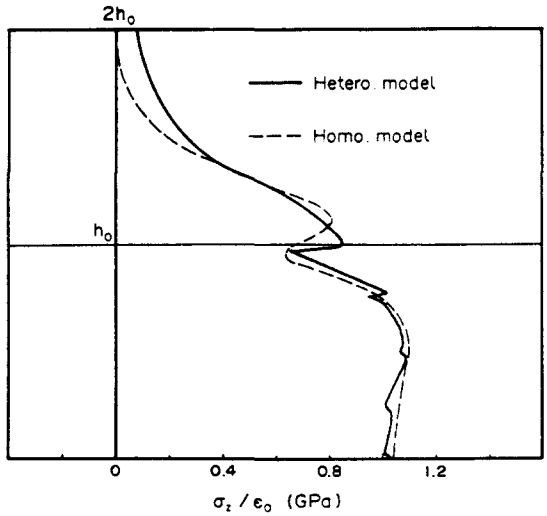

Fig. 21. Through-thickness distribution of σ_z near the free edge ($y/b = 0.9$) in $(0/90)_s$ laminate.

ined here drastically oversimplified the situation with respect to practical composites, it is believed that the main characteristics are not affected by the simplification.

For graphite/epoxy composite laminates in applications, the typical thickness of a ply in the laminates is 0.125 mm. It has been pointed out that the minimum dimension over which the effective moduli are applicable is about 0.045 mm. Hence, it is more rational to define interlaminar stresses from the heterogeneous representation of the material. However, even the simplest application of this model is rather complicated and time-consuming. The present analysis on the characteristics of interlaminar stress over the dimension of several times the fiber diameter indicates that the interlaminar stress response can be quantitatively the same for the heterogeneous and homogeneous models, when considering the integration of interlaminar stresses over a definite character length.

6. INTERLAMINAR STRESSES IN COMPOSITE LAMINATES UNDER BENDING

Considering a composite laminate subjected to bending in the x–z plane, from the symmetric and non-symmetric conditions of deformation, and the axial strain $\varepsilon_x = kz$ under simple bending, the following coefficients can be obtained,

$$C_1 = C_3 = C_4 = 0 \tag{23}$$

$$C_2 = k/S_{11}. \tag{24}$$

Then, the displacements in the laminate can be expressed as,

$$u = kxz + U(y,z) \qquad v = V(y,z) \qquad w = -\tfrac{1}{2}kx^2 + W(y,z). \tag{25}$$

An improved quasi-three-dimensional finite element method from Wang and Stango (1983) was used in the analysis. Similar to the previous analysis, the angle-ply $(\pm 45)_s$ and the symmetric cross-ply laminates were chosen as the investigative objects to examine the characteristics of interlaminar stress distributions in the regions close to the free edge. The dimensions and geometry of the laminates, as well as material constants typical of a high-modulus graphite/epoxy lamina, are the same as those in Wang and Stango (1983). Material and geometric symmetry conditions permit that only one half of the laminate cross-section be examined (Fig. 22 shows the finite element mesh). There are in total 216 elements and 715 nodes. Since the distributions of stress components, σ_x, σ_y, σ_z, and τ_{xy} are anti-symmetric

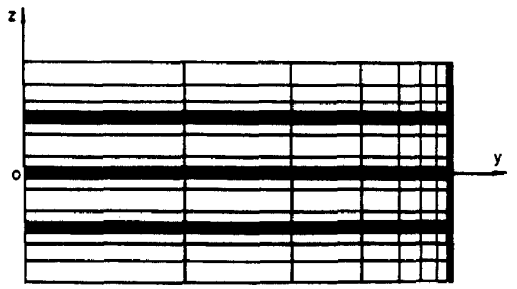

Fig. 22. Finite element mesh.

about the x–y plane, and τ_{xz}, τ_{yz}, symmetric, we only need to discuss the stress distributions in the upper one quarter region ($x \leqslant 0$, $y \leqslant 0$).

Results for $(\pm 45)_s$ laminate are shown in Figs 23–25. The distribution of interlaminar normal stress σ_z along the 45/−45 interface ($y = h_0$) is shown in Fig. 23. σ_z presents a compressive behavior near the free edge. Owing to the anti-symmetry of deformations, σ_z is a peeling stress and has a stress concentration in the interface ($y = -h_0$) near the free edge. Similarly, the interlaminar shear stress τ_{xz} increases rapidly near the free edge (Fig. 24). This indicates that τ_{xz} has a significant stress concentration near the free edge. The

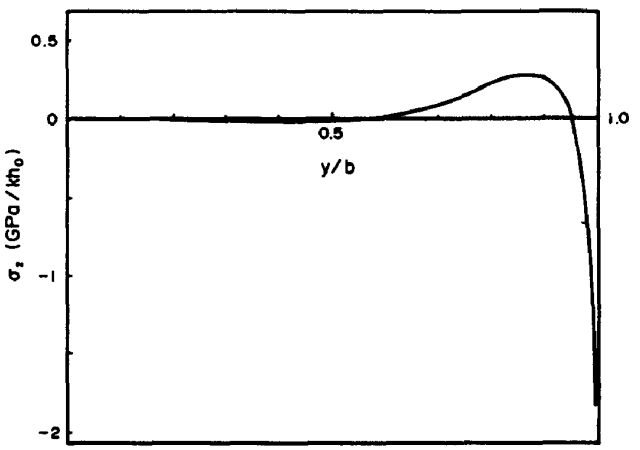

Fig. 23. Distribution of interlaminar normal stress σ_z along 45/−45 interface in $(\pm 45)_s$ laminate.

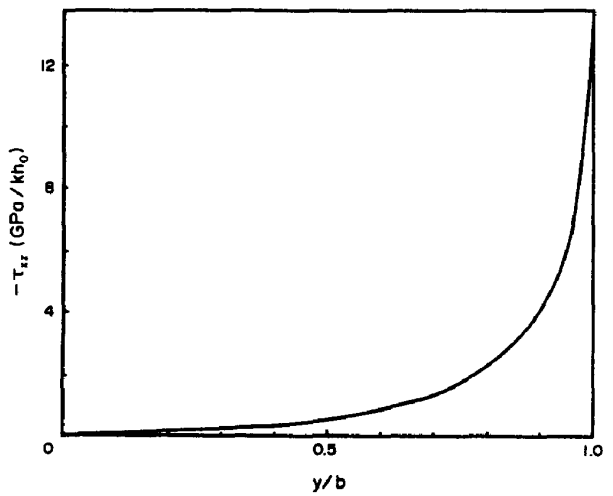

Fig. 24. Distribution of interlaminar shear stress τ_{xz} along 45/−45 interface in $(\pm 45)_s$ laminate.

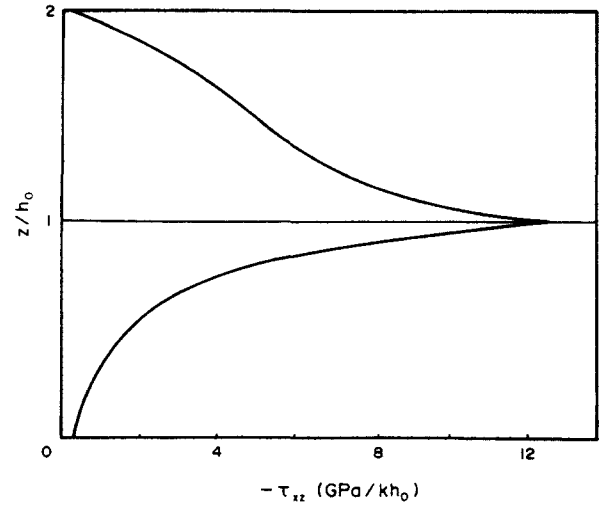

Fig. 25. Through-thickness distribution of τ_{xz} near the free edge ($y/b = 0.994$) in $(\pm 45)_s$ laminate.

distributions of σ_z and τ_{xz} along the interface ($y = h_0$) have characteristics similar to those in the laminate under uniform axial extension. A typical through-thickness distribution for τ_{xz} is shown in Fig. 25. It can be seen that near the free edge, shear stress τ_{xz} has its maximum value in the interface ($y = h_0$). It increases very sharply from the upper surface and the midplane of the laminate where it approaches zero.

Shown in Fig. 26 are distributions of interlaminar shear stress τ_{yz} along the 0/90 interface ($y = h_0$) for both $(0/90)_s$ and $(90/0)_s$ laminates. It is interesting to note that the distributions of interlaminar shear stress τ_{yz} for the $(0/90)_s$ and $(90/0)_s$ laminates are not mirror images of each other. The absolute values of τ_{yz} for $(0/90)_s$ laminate are obviously greater than those of $(90/0)_s$ laminate. Figure 27 shows the distributions of interlaminar normal stress σ_z along the 0/90 interface ($y = h_0$) for both $(0/90)_s$ and $(90/0)_s$ laminates. It is noticed that the stress distribution for $(90/0)_s$ laminate is not a mirror image of that for $(0/90)_s$ laminate. For $(0/90)_s$ laminate, σ_z increases rapidly near the free edge, which suggests a significant stress concentration. The distribution of σ_z for $(90/0)_s$ laminate shows an entirely different characteristic. The same trend was also found in the laminate under uniform axial extension. Through-thickness distributions of σ_z near the free edge for both $(0/90)_s$ and $(90/0)_s$ laminates are shown in Fig. 28. It is again noticed that the stress

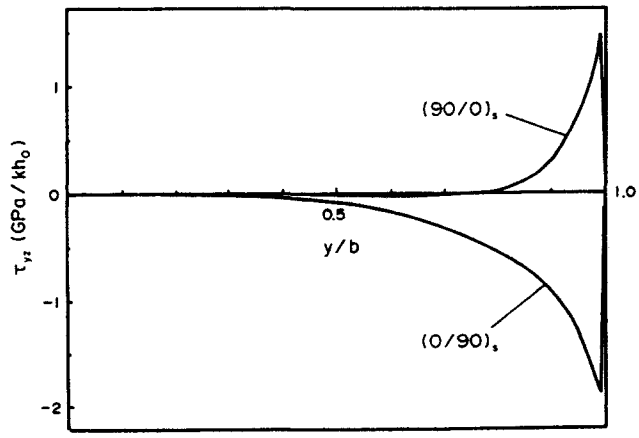

Fig. 26. Distributions of interlaminar shear stress τ_{yz} along 0/90 interface in $(0/90)_s$ and $(90/0)_s$ laminates.

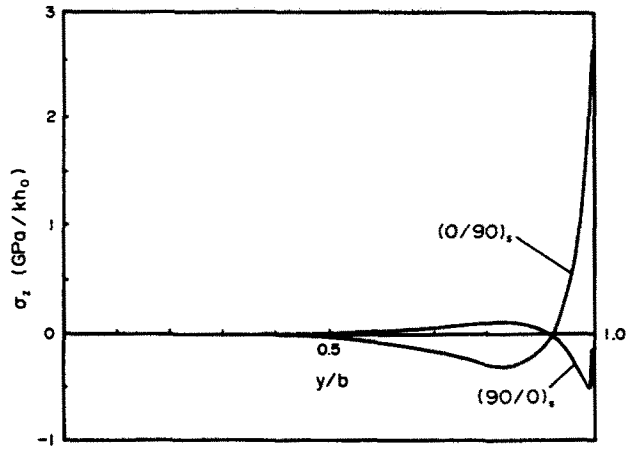

Fig. 27. Distributions of interlaminar normal stress σ_z along 0/90 interface in $(0/90)_s$ and $(90/0)_s$ laminates.

distribution for $(90/0)_s$ laminate is not a mirror image of that for $(0/90)_s$ laminate. It is also interesting to see that the maximum and minimum stresses do not occur at the 0/90 interface ($y = h_0$), but are located below the interface. For both laminates, σ_z approaches zero when approaching the midplane, which is different from that in the laminates under uniform axial extension.

By summarizing the results, the solutions indicate that complex stress states with a rapid change of gradients occur along the edge of composite laminates under bending. Owing to the anti-symmetry of deformations, the laminates are divided into two parts by the midplane. One half of the laminate is subjected to axial extension and another half is subjected to axial compression. In the part of the laminate subjected to axial extension, the distributions of interlaminar stresses have similar characteristics to those in the laminate under uniform axial extension. Near the free edge, interlaminar stresses also have significant stress concentration.

From the theory of linear elasticity, by superimposition, interlaminar stresses can be obtained for composite laminates under tension–bending coupling loading.

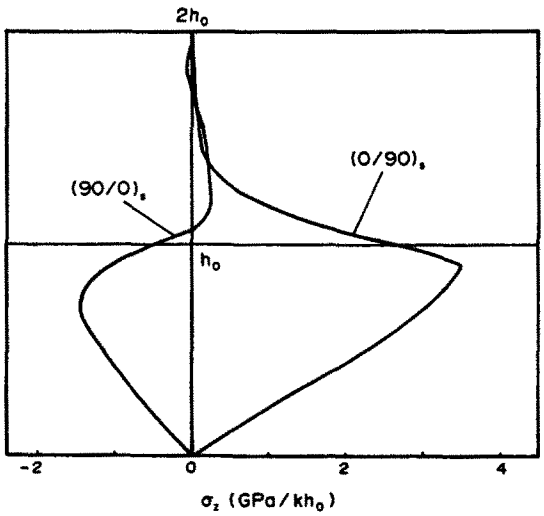

Fig. 28. Through-thickness distributions of σ_z near the free edge ($y/b = 0.994$) in $(0/90)_s$ and $(90/0)_s$ laminates.

7. CONCLUDING REMARKS

Some characteristics of the distribution of interlaminar stresses in composite laminates have been investigated. Based on the results, the following conclusions may be drawn.

(1) For the laminate model consisting of the non-linear response of the composite materials, the distribution of interlaminar stresses has similar characteristics to those in the linear elastic laminate model in many respects. Near the free edge, interlaminar stresses also have significant stress concentration. Under the assumption of small deformations, the presence of the non-linear response of the composite materials can reduce the stress concentration of interlaminar shear stresses to a certain degree, but has little effect on interlaminar normal stress. The linear elastic laminate model can be applied to evaluate the interlaminar stresses in composite laminates without any evident loss of accuracy.

(2) The strength of singularity of interlaminar stresses is quite weak. The dominant field of singular terms of interlaminar stresses may be ten orders smaller than that of stresses ahead of a crack tip in linear elastic fracture mechanics, and may be several orders smaller than the dimension of fiber diameters.

(3) When the macroscopically homogeneous model is applied to determine interlaminar stresses and other mechanical response in composite materials, the dimension over which the effective moduli are applicable should be considered. The effect of material heterogeneity on the distributions of interlaminar stresses is significant over the dimension of several times the fiber diameter. It is more rational to interpret the field values of interlaminar stresses by considering their integration over a definite character length.

(4) Complex stress states with a rapid change of gradients occur near the free edge in composite laminates under bending. Interlaminar stresses have significant stress concentration near the free edge. In the composite laminate under simple bending, the distribution of interlaminar stresses in the part of the laminate subjected to axial extension has characteristics similar to those in the laminate under uniform axial extension.

Acknowledgements—The author is grateful to professor Qing-zhi He and Professor Bing-xian Yang in Beijing Institute of Aeronautics and Astronautics for vigorous support and encouragement during the course of this study.

REFERENCES

Bar-Yoseph, P. and Pian, T. H. H. (1981). Calculation of interlaminar stress concentration in composite laminates. *J. Composite Mater.* **15,** 225–239.

Christensen, R. M. (1979). *Mechanics of Composite Materials.* John Wiley, New York.

Hahn, H. T. and Tsai, S. W. (1973). Nonlinear elastic behavior of unidirectional composite laminate. *J. Composite Mater.* **7,** 102–118.

Jones, R. M. (1975). *Mechanics of Composite Materials.* Scripta, Washington, D.C.

Lekhnitskii, S. G. (1963). *Theory of Elasticity of an Anisotropic Body.* Holden-Day, San Francisco.

Liu, G.-R. (1984). Experimental and theoretical studies on high-temperature behavior of graphite epoxy composite materials. S. M. thesis, Beijing Institute of Aeronautics and Astronautics.

Loo, T. T. (1986). On the nature of interlaminar edge stress in laminated composite structures. *Proc. Int. Symp. on Composite Materials and Structures.* 1986, Beijing, p. 801.

Pagano, N. J. (1978). Stress fields in composite laminates. *Int. J. Solids Structures* **14,** 385–400.

Pagano, N. J. and Rybicki, E. F. (1974). On the significance of effective modulus solutions for fibrous composites. *J. Composite Mater.* **8,** 214–228.

Pagano, N. J. and Soni, S. R. (1983). Global–local laminate variational model. *Int. J. Solids Structures* **19,** 207–228.

Pipes, R. B. and Pagano, N. J. (1970). Interlaminar stresses in composite laminates under uniform axial extension. *J. Composite Mater.* **4,** 538–548.

Puppo, A. H. and Evensen, H. A. (1970). Interlaminar shear in laminated composites under generalized plane stresses. *J. Composite Mater.* **4,** 204–220.

Raju, I. S. and Crews, J. H. Jr. (1981) Interlaminar stress singularities at a straight free edge in composite laminates. *Comput. Struct.* **14,** 21–28.

Rybicki, E. F. and Pagano, N. J. (1975). A study on the influence of microstructure on the modified effective modulus approach for composite laminates. *Proc.* 1975 *Int. Conf. Composite Mater.*, Vol. 2, p. 149.

Sih, G. C. and Liebowitz, H. (1968). Mathematical theories of brittle fracture. In *Mathematical Fundamentals of Fracture* (Edited by Liebowitz), Vol. 2. Academic Press, New York.

Spilker, R. L. and Chou, S. C. (1980). Edge effects in symmetric composite laminates: importance of satisfying the traction-free edge condition. *J. Composite Mater.* **14,** 2–20.

Tang, S. and Levy, A. (1975) A boundary layer theory—Part II: Extension of laminated finite strip. *J. Composite Mater.* **9,** 42–52.

Ting, T. C. T. and Chou, S. C. (1981a) Stress singularities in laminated composites. *Proc. Second U.S.A.-U.S.S.R. Symp. on Fracture of Composite Materials* (Edited by G. Sih and V. Tamuzs) p. 265. Martinus Nijhoff, Dordrecht.

Ting, T. C. T. and Chou, S. C. (1981b). Edge singularity in anisotropic composites. *Int. J. Solids Structures* **17**, 1057–1068.

Tsai, S. W. and Hahn, H. T. (1980). *Introduction to Composite Materials*. Technomic, Westport, CT.

Wang, A. S. D. and Crossman, F. W. (1977). Some new results on edge effects in symmetric composite laminates. *J. Composite Mater.* **11**, 92–106.

Wang, J. T. S. and Dickson, J. N. (1978). Interlaminar stresses in symmetric composite laminates. *J. Composite Mater.* **12**, 390–401.

Wang, S. S. and Choi, I. (1982a). Boundary-layer effects in composite laminates: Part 1—Free-edge stress singularities. *ASME J. Appl. Mech.* **49**, 541–548.

Wang, S. S. and Choi, I. (1982b). Boundary-layer effects in composite laminates: Part 2—Free-edge stress solution and basic characteristics. *ASME J. Appl. Mech.* **49**, 549–560.

Wang, S. S. and Stango, R. J. (1983). Optimally discretized finite elements for boundary-layer stresses in composite laminates. *AIAA Jl* **21**, 614–620.

Wang, S. S. and Yuan, F. G. (1983). A singular hybrid finite element analysis of boundary-layer stresses in composite laminates. *Int. J. Solids Structures* **19**, 825–837.

Whitney, J. M. and Riley, M. B. (1966). Elastic properties of fiber reinforced composite materials. *AIAA Jl* **4**, 1537–1542.

Xia, Yuan-Ming, Yang, Bao-Chang and Xu, Zhen (1986). Nonlinear constitutive relation of unidirectional composite laminate. *Acta Materiae Compositae Sinica* **3**(4), 44–49.

Ye, L. (1987). Analyses of interlaminar stresses and characterization of delamination in graphite/epoxy composite laminates. Ph.D. Dissertation, Beijing Institute of Aeronautics and Astronautics.

Zwiers, R. I., Ting, T. C. T. and Spilker, R. L. (1982). On the logarithmic singularity of free-edge stress in laminated composites under uniform extension. *ASME J. Appl. Mech.* **49**, 561–569.